

Morphological and functional reversal of phenotypes in a mouse model of Rett syndrome

Lianne Robinson,^{1,*} Jacky Guy,^{2,*} Leanne McKay,³ Emma Brockett,³ Rosemary C. Spike,³ Jim Selfridge,² Dina De Sousa,² Cara Merusi,² Gernot Riedel,¹ Adrian Bird² and Stuart R. Cobb³

¹ School of Medical Sciences, University of Aberdeen, Forresterhill, Aberdeen, AB25 2ZD, UK

² Wellcome Trust Centre for Cell Biology, School of Biological Sciences, University of Edinburgh, King's Buildings, Edinburgh, EH9 3JR, UK

³ Institute of Neuroscience and Psychology, College of Medical, Veterinary and Life Sciences, University of Glasgow, G12 8QQ, UK

*These authors contributed equally to this work.

Correspondence to: Stuart Cobb,
Institute of Neuroscience and Psychology,
College of Medical, Veterinary and Life Sciences,
University of Glasgow, Glasgow,
G12 8QQ, UK
E-mail: stuart.cobb@glasgow.ac.uk

Rett syndrome is a neurological disorder caused by mutation of the X-linked *MECP2* gene. Mice lacking functional *Mecp2* display a spectrum of Rett syndrome-like signs, including disturbances in motor function and abnormal patterns of breathing, accompanied by structural defects in central motor areas and the brainstem. Although routinely classified as a neurodevelopmental disorder, many aspects of the mouse phenotype can be effectively reversed by activation of a quiescent *Mecp2* gene in adults. This suggests that absence of *Mecp2* during brain development does not irreversibly compromise brain function. It is conceivable, however, that deep-seated neurological defects persist in mice rescued by late activation of *Mecp2*. To test this possibility, we have quantitatively analysed structural and functional plasticity of the rescued adult male mouse brain. Activation of *Mecp2* in ~70% of neurons reversed many morphological defects in the motor cortex, including neuronal size and dendritic complexity. Restoration of *Mecp2* expression was also accompanied by a significant improvement in respiratory and sensory-motor functions, including breathing pattern, grip strength, balance beam and rotarod performance. Our findings sustain the view that *MECP2* does not play a pivotal role in brain development, but may instead be required to maintain full neurological function once development is complete.

Keywords: Rett syndrome; *MECP2*; morphology; motor function; breathing

Introduction

Rett syndrome (MIM 312750) is a severe mental retardation syndrome that is characterized by a constellation of distinctive clinical features, including developmental regression, with accompanying loss of hand skills, mobility and speech (Neul *et al.*, 2010). Microcephaly, stereotypic hand movements, respiratory abnormalities, seizures, scoliosis, growth deficits and hypotonia are also prevalent. The vast majority of cases with Rett syndrome

result from sporadic mutations in the X-linked gene *MECP2*, which encodes methyl-CpG-binding protein 2 (MeCP2) (Amir *et al.*, 1999). Most pathogenic mutations in *MECP2* cause Rett syndrome in heterozygous females, while males do not normally survive infancy (Moretti and Zoghbi, 2006). Rett syndrome can be modelled using *Mecp2* knockout mice that recapitulate many of the key clinical signs (Chen *et al.*, 2001; Guy *et al.*, 2001). Male *Mecp2*-null mice demonstrate apparently normal early development before the onset of overt signs at ~6 weeks of age leading

to death by 20 weeks. Heterozygous female mice, on the other hand, show delayed onset of overt signs (4–12 months) followed by stabilization. Neurobiological changes in the *Mecp2*-null brain appear to be complex. At the cellular level, studies show rather subtle changes in neuronal electrical properties (Dani *et al.*, 2005; Taneja *et al.*, 2009; Kline *et al.*, 2010), but more overt changes in synaptic function including reduced synaptic plasticity (Asaka *et al.*, 2006; Moretti *et al.*, 2006; Guy *et al.*, 2007; Nelson *et al.*, 2008; Weng *et al.*, 2011) and changes in basal inhibitory and excitatory synaptic transmission (Dani *et al.*, 2005; Medrihan *et al.*, 2008; Nelson *et al.*, 2008; D'Cruz *et al.*, 2010; Kline *et al.*, 2010; Maliszewska-Cyna *et al.*, 2010). Anatomical studies show changes in synaptic connectivity and neuronal structure (Belichenko *et al.*, 1994, 1997, 2008, 2009a,b; Armstrong *et al.*, 1995, 1998, 2005; Kishi and Macklis, 2004; Chao *et al.*, 2007) while at the network level there is altered excitability (Zhang *et al.*, 2008; D'Cruz *et al.*, 2010).

Despite these pervasive defects, activation of a silenced *Mecp2* allele in ~80% of neurons after the onset of Rett syndrome-like signs reverses observed defects in both males and females (Guy *et al.*, 2007). Reversibility appears to question the straightforward categorization of Rett syndrome as a neurodevelopmental disorder, as it suggests that MeCP2 deficiency during brain development does little lasting damage. A conservative interpretation might be, however, that reversal is superficial, meaning that underlying neurological defects persist in the 'reversed' mice. Phenotypic characterization by Guy *et al.* (2007) used semi-quantitative observational scoring for survival, gait, breathing, tremor, mobility and general condition (an exception was quantitatively robust reversal of defective hippocampal long-term potentiation). Here, we ask whether underlying features of brain morphology and sensory-motor function are rectified by late activation of *Mecp2*. We find that activation in ~70% of neurons leads to significant improvement in almost all features, suggesting that phenotypic reversal is profound.

Materials and methods

Mice

Mecp2^{Stop/+} mice in which the endogenous *Mecp2* allele is silenced by a targeted stop cassette (*Mecp2*^{tm2Bird}, Jackson Laboratories Stock No. 006849) were crossed with hemizygous *CreESR* transgenic mice (*CAG-Cre/ESR1**, Jackson Laboratories Stock No. 004453) to create experimental cohorts (Guy *et al.*, 2007). Animals were bred on an inbred C57BL6/J background for neuronal morphology experiments. As breeding performance of *Mecp2*^{+/-} animals is extremely poor on a C57BL6 inbred background, a breeding strategy of crossing C57BL6/J/CBA F1 animals and using the F2 offspring was adopted to facilitate the generation of large cohorts of mice for functional studies (behavioural and respiratory phenotyping). The genotype of the mice was determined by polymerase chain reaction (Guy *et al.*, 2007). Mice were housed in groups with littermates, maintained on a 12-h light/dark cycle and provided with food and water *ad libitum*. Experiments were carried out in accordance with the European Communities Council Directive (86/609/EEC) and a project licence with local ethical approval under the UK Animals (Scientific Procedures) Act (1986).

Immunoblotting, polymerase chain reaction and Southern blots

Protein extracts for western blot analysis were prepared from snap-frozen brains that had been hemisected prior to freezing. Half brains were homogenized in a Dounce homogenizer in 750 µl ice-cold NE1 buffer [20 mM HEPES pH 7.9, 10 mM KCl, 1 mM MgCl₂, 0.1% Triton X-100, 0.5 mM DTT, 20% glycerol, protease inhibitor cocktail (Roche)]. Samples were treated with 750 U Benzonase® (Sigma) for 15 min at room temperature. An equal volume of 2 × loading buffer was added (125 mM Tris-Cl pH 6.8, 20% glycerol, 0.01% bromophenol blue, 2% β-mercaptoethanol) and the samples were vortexed, snap-frozen and boiled for 3 min.

Proteins were resolved by sodium dodecyl sulphate polyacrylamide gel electrophoresis and transferred to polyvinylidene fluoride membrane. Membranes were hybridized with a monoclonal antibody recognizing the C-terminus of MeCP2 (Sigma, M6818) and developed by quantitative infrared imaging (LI-COR Odyssey®, LI-COR Biosciences). Intensity of protein bands was quantified using LI-COR Odyssey® software.

Recombination of the *Mecp2*^{Stop} allele was quantified as described previously (Guy *et al.*, 2007) using the remaining half of each snap-frozen brain. When brains were to be used for Golgi–Cox staining, the front and rear portions of the brain were removed by coronal cuts for Southern analysis, before the central portion including the cortex was processed further.

Scoring of symptoms

Mice were observed and scored on a weekly basis for a number of symptoms arising from MeCP2 deficiency. These weekly assessments of cardinal Rett syndrome-like features generated a semi-quantitative measure of symptom status. Each of six signs (mobility, gait, hindlimb claspings, tremor, breathing and general condition) was scored as 0 (absent or as wild-type), 1 (symptom present) or 2 (symptom severe) as previously described (Guy *et al.*, 2007). The aggregate score was used to determine when animals should commence tamoxifen treatment or be culled for humane reasons.

Tamoxifen treatment

Tamoxifen (Sigma) was dissolved by sonication in corn oil (Sigma) at a concentration of 20 mg/ml aliquoted and stored at –20°C until required. Tamoxifen (100 mg/kg) was administered via intraperitoneal injection at an injection volume of 5 ml/kg body weight. A treatment regime of one injection of tamoxifen per week for 3 weeks followed by four daily injections on consecutive days in the fourth week was employed. For behavioural studies tamoxifen treatment was initiated once all animals had completed the initial behavioural screens (see below) and Stop/Cre lines displayed a group mean of 5/6 according to the severity scale of symptoms (see above). Animals for neuronal morphology and respiratory phenotyping were individually monitored and tamoxifen treatment started once the aggregate symptom score was at least 6. Wild-type controls were treated with tamoxifen in parallel with their littermates.

Neuronal morphology

Golgi–Cox staining was performed using the FD Rapid GolgiStain kit (FD NeuroTechnologies). Male mice (age 9–21 weeks, Supplementary Fig. 1) were killed by cervical dislocation and brains rapidly removed,

rinsed briefly in water and processed according to the manufacturer's protocol, and sections were cut at 240 µm thickness on a cryostat. Pyramidal neurons from layer II/III of primary motor cortex (M1) were observed by an investigator blind to the genotype under a Nikon Eclipse E400 microscope and reconstructed on a 2D plane using a drawing tube under the $\times 40$ objective lens. To ensure relative neuron completeness, cells were selected that were located close to the centre of the section and had pyramidal cell morphology with the primary apical dendritic trunk orientated in line with the plane of the section. Analysis was limited to a 220 µm radius, and cells with significant processes cut at the surface of the section were excluded from the analysis. Despite the most distal aspects of the dendritic arbor not being sampled with this approach, the method nevertheless allows the comparison of salient features of dendritic morphology in randomly sampled neurons from both genotypes and treatment groups before or following tamoxifen treatment. Branching was studied by Sholl analysis (Kishi and Macklis, 2004; McNair *et al.*, 2010). For spine density analysis, segments of secondary oblique dendrites in hippocampal area CA1 (chosen due to the homogenous defined synaptic input and non-tapering dendrites), were reconstructed using $\times 100$ oil immersion lens and the number of spines per unit length calculated (McNair *et al.*, 2010). Morphological data were initially evaluated using unpaired *t*-tests and a secondary analysis conducted by ANOVA with Tukey's *post hoc* test where appropriate. For Sholl analysis, groups were compared using a repeated measures two-way analysis of variance (ANOVA) with Tukey's *post hoc* analysis.

Respiratory phenotyping

Changes in respiratory frequency (mean \pm SD) were recorded *in vivo* during periods of quiet restfulness by using whole body plethysmography (Buxco Electronics Inc.; Elphy software, INAF, CNRS). Respiratory baseline parameters were established for each mouse on three sequential days prior to tamoxifen treatment and again on three sequential days ~ 5 weeks after the end of treatment.

The plethysmographic chamber (700 ml) was connected to a differential pressure transducer (Model DP103-4, Validyne Engineering), which measured pressure fluctuations within the closed chamber relative to a reference chamber of the same volume. During each 2 min recording session the chamber was hermetically sealed and temperature was continuously recorded and maintained between 27 and 28°C. Data from each 2 min recording were analysed using Spike 2 (Cambridge Instruments). The breath by breath analysis to determine baseline frequency and variability was performed on data recorded during periods of quiet wakefulness and excluded periods of apnoea (cessation of breathing, more than three missed breaths), hyperpnoea (rapid breathing) and movement. The number of sigh-like breaths was counted in each recording. Each mouse (Wild-type/Cre $n = 11$; Stop/Cre $n = 10$) was exposed to the protocol three times before and after tamoxifen treatment and the results of these sessions averaged. Data were statistically evaluated using two-way ANOVA followed where appropriate ($P < 0.05$) by Tukey's *post hoc* test.

Behavioural phenotyping

A typical experiment consisted of an initial assessment of the mice to define early mild symptoms at 5–6 weeks of age followed by tamoxifen treatment and retesting 5–6 weeks after treatment in the same protocols (Supplementary Figs 2 and 3). The low survival rate in Stop mice precluded retesting after treatment (no gene rescue) so that behavioural assessment was performed on two cohorts of male mice of

Stop and Stop/Cre genotype and only survivors that completed the protocols pre- and 5–6 weeks post-treatment are considered. Cohort 1 (Wild-type/Cre $n = 25$; Stop/Cre $n = 17$) was tested in sequence for grip strength, on the rotarod, balance beams and CatWalk (see below). Cohort 2 (Wild-type/Cre $n = 7$; Stop/Cre $n = 9$) performed a short swim test.

Grip strength

The forelimb grip strength was determined using a grip-strength meter (Ugo Basile). Each mouse grasped the trapeze and upon gentle pulling of the tail, maximal grip strength was automatically recorded. Each animal performed two trials (intertrial interval 2 min).

RotaRod

An automated 4-lane accelerating RotaRod (TSE) was used to examine motor learning and motor coordination. Testing (pre- and post-treatment) consisted of four trials per day for two consecutive days with intertrial intervals of 2–3 min. For each trial, the mouse was placed on the rotating rod (1 rpm). The rod was accelerated from 1 to 45 rpm over the trial time of 5 min. Trials were terminated when animals fell off the rod or the maximum time was achieved. Lanes were allocated following a Latin square design to counterbalance for both rod position and time of testing.

Balance beam

Sensory-motor coordination was tested using balance beams (50 cm length; 28, 11 or 5 mm cross-section; 30% incline). Each mouse was given two trials per beam. Latency to traverse the beam was scored and averaged. Failure to traverse the beam during the allotted time terminated the trial and the maximum time (30 s) was recorded. As for all behavioural tests, apparatus was wiped with 70% ethanol between animals.

CatWalk

Gait analysis was performed on walking mice using the CatWalk (Noldus; version 7.1). Five trials per mouse with a maximum of 10 s to traverse the glass plate were administered. Data recorded include paw position, timing, pressure and dimensions of each footfall, which enabled calculation of stride length and paw distance.

Swim test

The swim test was performed using an open-field water maze (150 cm diameter). Mice were released facing the wall of the pool and allowed to swim for 30 s after which time they were removed and returned to their home cages. The swim trajectory and speed of the mouse were recorded and tracked by an overhead video camera and tracking software Anymaze (Ugo Basile).

Data handling and analysis

For all behavioural data, Gaussian distribution was confirmed, before group means for each genotype and time point (pre- and post-treatment) were analysed by two-way ANOVAs followed, where appropriate, by Bonferroni *post hoc* tests using Prism 5.0 (Graphpad). Alpha was always set to 0.05. For simplicity, only reliable differences are indicated.

Results

Silencing and rescue of MeCP2 expression in *Mecp2*^{Stop/y}; *CreESR* mice

severe, 3.8% wild-type level). Although a small number of *Stop/y* animals in this study showed extended survival compared with that reported previously (Guy *et al.*, 2007), this is likely due to the use of a mixed C57BL6/CBA F2 genetic background in the current study, rather than the presence of elevated MeCP2 levels in these animals. Given the similarity between the phenotypes of *Stop/y* and *Mecp2*-null mice, we conclude that the ~25–100-fold reduction in MeCP2 abundance is approximately equivalent to the deletion of the *Mecp2* gene. Activation (de-silencing) of the *Mecp2*^{Stop} allele was achieved by tamoxifen injection of mice, leading to translocation of the Cre-ESR fusion protein into the nucleus and excision of the Stop cassette. Southern blot analysis of 61 treated *Stop/y,Cre* mice revealed the recombination frequency in brain to be $69.8 \pm 1.3\%$ (range 52–83%; Fig. 1B). We also tested levels of MeCP2 protein following tamoxifen treatment by quantitative immunoblotting and found that treated *Stop/y,Cre* mice showed substantially increased levels of MeCP2 (Fig. 1C).

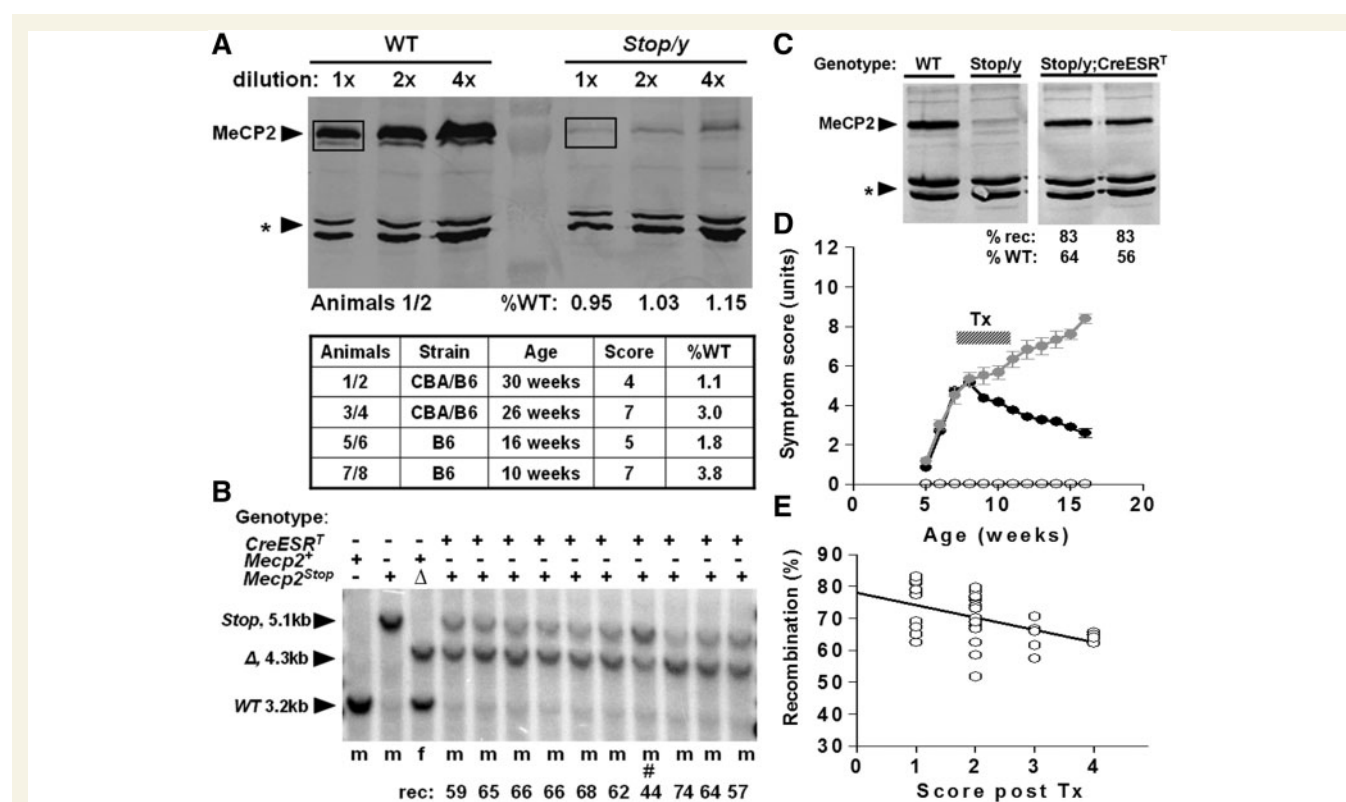


Figure 1 Silencing and rescue of MeCP2 expression in *Mecp2^{Stop/y,Cre}* mice. **(A)** Quantitative western blots showing brain MeCP2 expression in wild-type (WT) and *Stop/y* males. Western blotting of whole brain extracts from wild-type and *Stop/y* littermates was used to quantify the amount of MeCP2 produced by the *Stop* allele. The amount of MeCP2 (boxed) was normalized to a non-specific cross-reacting band (asterisk) as a loading control. MeCP2 was measured for four *Stop/y* animals of different strain backgrounds, ages and aggregate symptom scores. **(B)** Southern blot showing recombination of the *Stop/y* allele (5.1 kb) to delete the *Stop* cassette (open triangle, 4.3 kb) after tamoxifen (Tx) treatment. All animals received the same tamoxifen-treatment regimen apart from #, which died soon after treatment started. **(C)** Representative western blot showing levels of MeCP2 protein in brains of wild-type, *Stop/y* and two tamoxifen-treated *Stop/y;CreESR^T* animals. Recombination levels and the amount of protein relative to wild-type are shown. **(D)** Time plot showing phenotypic scores (see ‘Materials and methods’ section) for wild-type (open circle), *Stop/y* (black filled circles) and *Stop/y,Cre* mice (grey filled circles). Note the rapid symptom progression followed by a sustained improvement in symptom score following tamoxifen in the *Stop/y,Cre* cohort. **(E)** Recombination levels in brains of *Stop/y,Cre* mice showing relationship between higher recombination efficiency and milder symptom score at end of study.

To recapitulate previous studies, we utilized male mice that were hemizygous for the *Mecp2*^{Stop} allele. Although a backcrossed C57BL6 background was used in our previous study (Guy *et al.*, 2007), the poor breeding performance of these mice made it necessary to use an outbred genetic background for the aspects of this study requiring large cohorts of animals (breathing and behavioural analysis). Consistent with earlier data, however, these mice developed a range of overt signs including hypoactivity, irregular breathing, gait disturbances and hind limb claspings from around post-natal week 4–8. They also showed greatly reduced survival over the 16-week experiment. Reactivation of the *Mecp2* allele in the *Stop/y; CreESR* line following tamoxifen treatment led to a sustained reduction in symptom severity (Fig. 1D) and increased survival as reported previously (Guy *et al.*, 2007). In contrast, the *Stop/y* cohort, which lacked Cre and was therefore unable to respond to tamoxifen, showed progressively increasing phenotypic severity leading to premature death. All scoring was performed blind to genotype and treatment. *Post hoc* analysis revealed a negative correlation between final phenotypic scores and the level of MeCP2 activation as measured by recombination levels in *Stop/y; Cre* mice (Fig. 1E, linear regression, $R^2 = 0.23$, slope $\neq 0$, $P < 0.005$). This indicates a causal relationship between the degree of symptom improvement and the number of cells expressing MeCP2 post-treatment.

Restoration of MeCP2 reverses structural deficits in cortical neurons

Severe motor impairments are a key feature of Rett syndrome (Nomura and Segawa, 1992) and are also seen in mice lacking MeCP2 (Chen *et al.*, 2001; Guy *et al.*, 2001, 2007; Luikenhuis *et al.*, 2004). Corresponding structural abnormalities have also been reported in motor cortex of patients with Rett syndrome and *Mecp2*-null mice, including a thinning of the cortical layers and a reduction in neuronal size and complexity (Armstrong *et al.*, 1995, 1998; Kishi and Macklis, 2004; Belichenko *et al.*, 2009a,b). We wanted to determine whether gross phenotypic improvements seen previously upon reactivation of *Mecp2* in mice (Guy *et al.*, 2007) are accompanied by morphological changes within the adult nervous system. We focused our investigations on the primary motor cortex. Male *Stop/y* mice and wild-type littermate controls were sampled for morphometric analysis at 3 months of age, at which time the mutant mice displayed overt Rett-like signs (gross phenotype score = 4.3 ± 0.6). At the same time, an age-matched cohort of mice, including littermates of the *Stop/y* mice, which also carried the Cre transgene (*Stop/y; Cre*, mean symptom score = 4.3 ± 0.3), were given tamoxifen to instigate *Mecp2* gene activation (de-silencing). These mice together with tamoxifen treated wild-type controls were then sampled for morphological analyses at 8–10 weeks following tamoxifen treatment. By this time the mean symptom score had reduced to 1.8 ± 0.3 in the *Stop/y; Cre* cohort. Unreactivated hemizygous *Stop/y* mice did not survive to this time point and were therefore unavailable as a matched control group.

Brains were Golgi stained and corresponding sections from each mouse ($n = 16$, four per group) assessed for a range of gross

measures including neocortical thickness and thickness of the underlying corpus callosum (Fig. 2A and B). A random sample of layer 2/3 pyramidal cells ($n = 210$) was reconstructed by camera lucida to assess a range of cellular parameters, including soma size and various dendritic measures (Fig. 2C–E). Untreated *Stop/y; Cre* mice displayed significantly reduced thickness of motor cortex ($83 \pm 2.6\%$ of control) and underlying white matter tract ($83 \pm 1.4\%$ of control). At the cellular level, layer 2/3 pyramidal cells showed a consistent reduction in soma size ($83 \pm 2.7\%$ of control), dendritic complexity and dendritic length, consistent with previous reports (Armstrong *et al.*, 1995; Kishi and Macklis, 2004) (Fig. 2C–E). To quantify synaptic measures, secondary oblique dendrites in hippocampal area CA1 were assessed to reveal a significant reduction in spine density ($78 \pm 2.7\%$ of control; $n = 51$ –65 dendritic segments per group; Fig. 2E). Following tamoxifen treatment, all measured variables showed a trend towards wild-type levels. With the exception of cortical thickness, all parameters were not significantly different from their respective age-matched, wild-type controls (Fig. 2E; *t*-test, all P -values > 0.05) at 8–10 weeks post-tamoxifen. Further analysis confirmed a significant interaction between genotype and treatment for motor cortex soma size, dendritic length and hippocampal spine density (ANOVA, comparison of untreated *Stop/y*, treated *Stop/y; Cre* and corresponding wild-type mice, $P < 0.05$; Tukey's *post hoc* comparison showing a significant treatment effect (all P -values < 0.05). While overall dendritic complexity showed a significant genotype difference between wild-type and both untreated and treated *Stop/y; Cre* mice (ANOVA, $P < 0.05$), neurons from untreated *Stop/y* mice showed significantly reduced values of dendritic complexity across 6 of 11 measured Sholl radii, whereas the post-treatment cohort differed from wild-type at only 2 of the 11 Sholl radii. These data provide evidence that restoration of *Mecp2* to ~70% of cells leads to the normalization of morphological changes caused by earlier deficiency of *Mecp2*.

Normalization of respiratory measures upon Mecp2 reactivation

In addition to severe motor deficits, patients with Rett syndrome and *Mecp2*-deficient mice display a pronounced respiratory phenotype including apnoeas and irregular breathing patterns (Katz *et al.*, 2009). We therefore tested the propensity for respiratory phenotype reversal upon reactivation of *Mecp2* in adult mice by recording breathing patterns before and after tamoxifen treatment. In *Stop/y; Cre* mice, respiratory patterns varied within and between recordings, this variability was characterized by periods of hyperpnoea-like breathing (increased frequency) followed by periods of slow breathing due to prolonged expirations (Fig. 3A and C). Despite this, there was no significant difference in average respiratory frequency *per se* between *Stop/y; Cre* mice [310 ± 76 breaths per minute (bpm), $n = 8$] and wild-type littermate controls (305 ± 60 bpm, $n = 11$, $P > 0.05$; Fig. 3D) prior to tamoxifen treatment. In contrast, the coefficient of variation of respiratory frequency (CV%) was significantly higher in *Stop/y; Cre* mice ($32 \pm 17\%$, $n = 8$) when compared with wild-type littermate

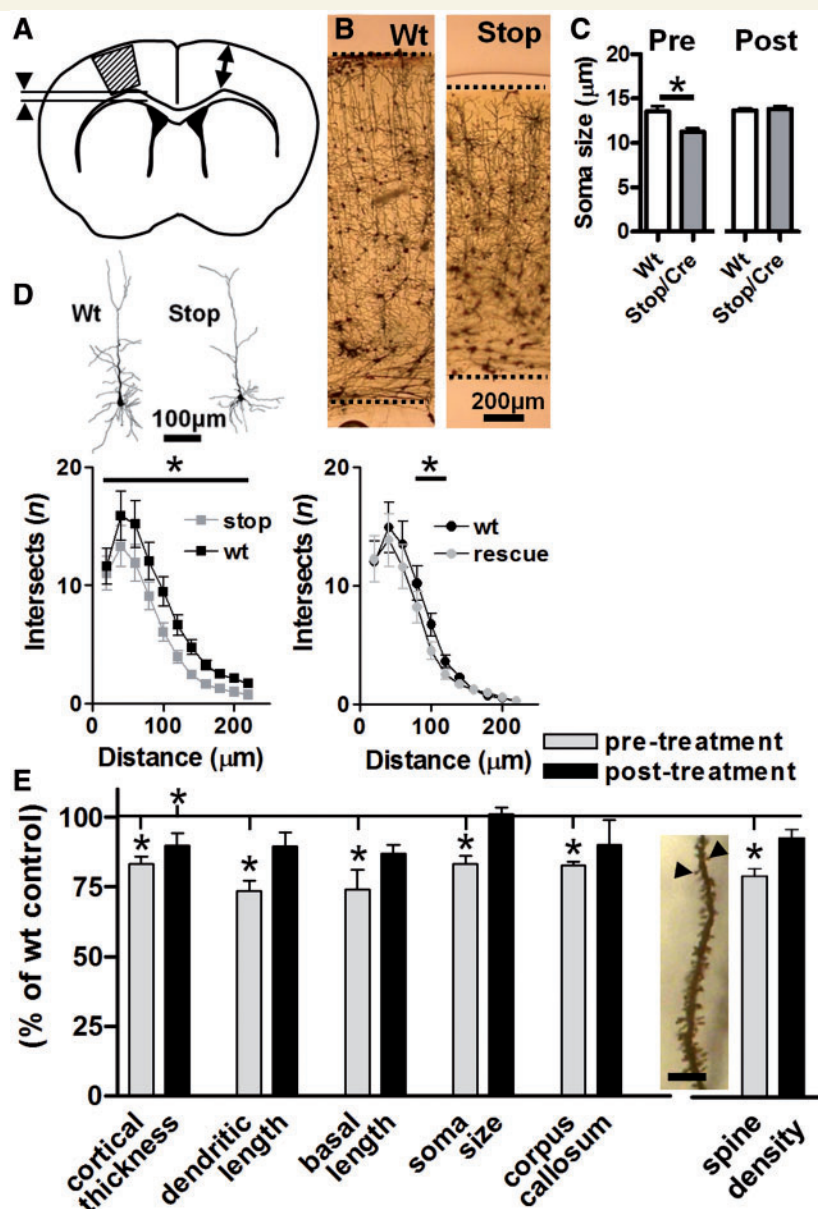


Figure 2 Quantitative assessment of neuronal morphology in primary motor cortex following *Mecp2* reactivation. (A) Golgi labelled brain sections from wild-type (Wt) and *Stop/y,Cre* mice were sampled for gross measures of cortical thickness (arrows) and corpus callosum (arrowheads) as well as layer 2/3 pyramidal cell morphology within primary motor cortex (hatched area). Analysis revealed reduced cortical thickness (B, representative micrographs) and reduced soma diameter (C) in *Stop/y,Cre* untreated mice. (D) Quantitative assessment of reconstructed cells (representative examples shown) by Sholl analysis ($n = 50$ – 60 cells/four animals per group, total 210 cells) revealed reduced dendritic branching complexity in *Stop/y,Cre* mice compared with wild-type littermate controls at Sholl radii 20–140 μm from soma. At 8–10 weeks following tamoxifen treatment, overall branching complexity was still reduced ($P < 0.05$, ANOVA followed by Tukey A *post hoc* analysis) compared with wild-type but this difference was restricted to Sholl radii between 60–80 μm from soma. (E) Pooled data revealed a significant (*t*-test comparison with age-matched wild-type, $*P < 0.05$) reduction in all parameters measured (cortical thickness, total dendritic length, length of basal dendritic tree, soma diameter and corpus callosum thickness) in *Stop/y,Cre* mice compared with wild-type littermates. A reduction was also observed in spine density (measured in primary oblique dendrites of hippocampal CA1 pyramidal cells as shown in insert; scale = 10 μm). Analysis of tamoxifen treated (rescued) mice revealed no significant difference from their appropriate littermate controls with the exception of cortical thickness, which remained significantly reduced compared with age-matched controls.

controls ($16.8 \pm 8.2\%$, $n = 11$, $P < 0.05$; Fig. 3E). Following tamoxifen treatment the breathing pattern in *Stop/y,Cre* mice became more regular with fewer periods of alternating fast and slow breathing. Indeed, there remained no significant difference in

respiratory frequency between genotypes (*Stop/y,Cre* = 283 ± 65 bpm, $n = 8$ versus wild-type littermates = 286 ± 71 bpm, $n = 11$, $P > 0.05$) whereas the frequency variability reverted to wild-type levels in treated *Stop/y,Cre* mice (post-tamoxifen *Stop/y,Cre*

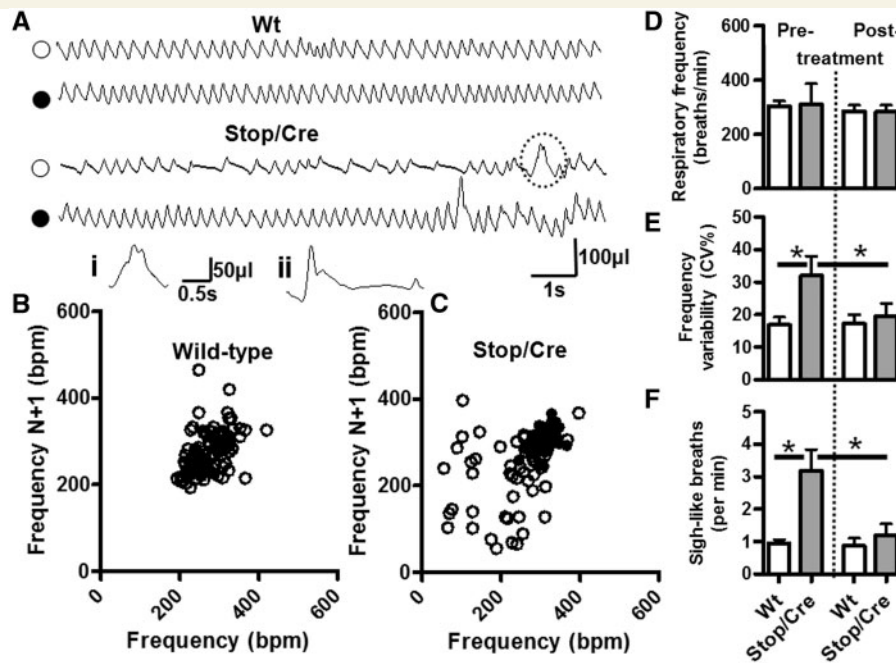


Figure 3 Improved respiratory pattern following delayed activation of *Mecp2*. (A) Representative plethysmographic traces of wild-type (Wt) and *Stop/y,Cre* mice before (open symbols) and 5 weeks following tamoxifen treatment (filled symbols). Pre-tamoxifen treatment, the respiratory trace from a *Stop/y,Cre* mouse is characterized by periods of fast to normal frequency breathing interspersed with periods of slow breathing due to prolonged expirations. Post-tamoxifen treatment, the respiratory trace from the *Stop/y,Cre* mouse is similar to wild-type. Insert (i) is an illustration of the sigh-like breath indicated by the dashed lines in the *Stop/y,Cre* breathing trace. Insert (ii) is an example of a typical sigh, large amplitude breath followed by a prolonged expiratory pause. These sigh-like breaths were highly prevalent in *Stop/y,Cre* respiratory traces. Plotting the respiratory traces as Poincaré plots (B, wild-type; C, *Stop/y,Cre*) shows an increased scatter, thus increased variability of breathing pattern, in *Stop/y,Cre* pre-tamoxifen treatment (open symbols) when compared with post-tamoxifen *Stop/y,Cre* and with wild-type. Overall, there was no significant difference in average baseline (i.e. apnoea-free segments) respiratory frequency (D) between groups (wild-type, $n = 11$; *Stop/y,Cre* $n = 8$); however the variability in respiratory frequency (E) was significantly increased in *Stop/y,Cre* mice pre-tamoxifen treatment when compared with post-tamoxifen treatment and wild-type. Pre-tamoxifen treatment, *Stop/y,Cre* mice exhibited an increased number of sigh-like bpm [F, A(i) and A(ii)], which was significantly reduced post-tamoxifen treatment ($*P < 0.05$).

CV% = $20 \pm 11\%$, $n = 8$ versus post-tamoxifen wild-type littermates = $17 \pm 9\%$, $n = 11$, $P > 0.05$) with *post hoc* tests indicating a significant improvement in frequency variability from pre- to post-treatment in *Stop/y,Cre* mice ($P < 0.05$).

We noted that *Stop/y,Cre* mice displayed an increased occurrence of sigh-like breaths [Fig. 3A(i), A(ii) and F]. More specifically these were large amplitude inspirations followed by a typical post-sigh expiratory pause, or large amplitude inspirations followed rapidly by a second smaller breath during the expiratory phase with no subsequent post-sigh expiratory pause. The occurrence of sigh-like breaths was significantly increased in *Stop/y,Cre* mice (3.2 ± 0.7 sighs per min, $n = 8$) compared with wild-type littermate controls (1.0 ± 0.1 sighs per min, $n = 11$). Post-tamoxifen, the occurrence of sighs decreased in *Stop/y,Cre* mice (1.2 ± 0.3 sighs per min, $n = 8$) similar to that seen in wild-type (0.9 ± 0.2 sighs per min, $n = 11$), again showing a significant treatment effect in *Stop/y,Cre* mice ($P < 0.05$). Our findings provide unequivocal quantitative evidence for functional improvement in specific breathing phenotypes following delayed activation of *Mecp2*.

Improvement in sensory-motor tasks after gene rescue

We next focused on the reversibility of sensory-motor skills. Overt neurological symptoms were quantified in different cohorts using a battery of sensorimotor tests. Tests were first conducted at a time when disease symptoms in *Stop/y,Cre* mice appeared mild–moderate (4–6 weeks of age). The *Mecp2* gene was then activated and animals were retested 5 weeks later. Sensory-motor abilities were assessed on round and rectangular balance beams (Fig. 4A). Data pooled for beam size clearly revealed deficient performance compared with wild-type in *Stop/y,Cre* mice prior to treatment [Fig. 4A(i)]. Notably, MeCP2-deficient mice found smaller diameter beams difficult (interaction between beam size and genotype: $P < 0.05$). Upon treatment, *Stop/y,Cre* mice improved on all beam sizes ($P < 0.05$; *post hoc* Bonferroni: all $P < 0.05$) and no longer differed from wild-type controls at the large diameter beams (28 mm), indicating motor improvement after tamoxifen treatment. *Stop/y,Cre* animals still found the smaller beam sizes very challenging [Fig. 4A(ii)]. Wild-type mice also improved their

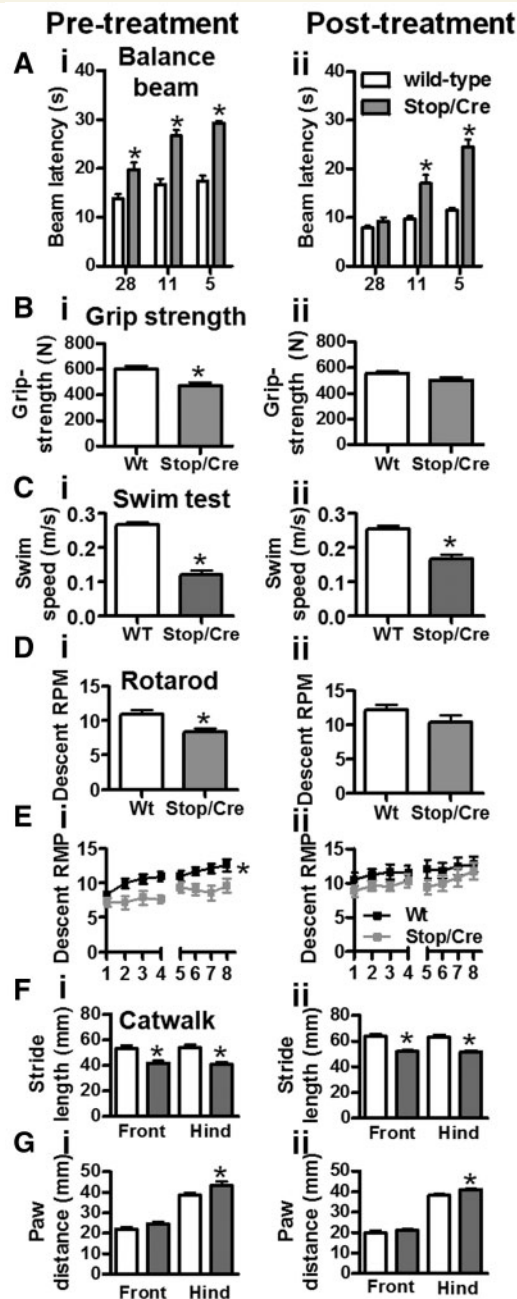


Figure 4 Improvement in balance and motor function following activation of *Mecp2*. [A(i)] Both *Stop* ($n = 24$) and *Stop/y,Cre* ($n = 17$) mice displayed similar impairment in balance beam performance compared with wild-type pretreatment at all beam widths tested (5–28 mm round and rectangular beams combined). [A(ii)] Following tamoxifen treatment, *Stop/y,Cre* ($n = 17$) mice improved performance when tested on the large (28 mm) beams, but remained significantly impaired relative to wild-type in the narrower beams. Note that impairment became more pronounced as the task was made more challenging with narrower beams. [B(i)] Grip strength at pretreatment showed significant impairment in *Stop/y,Cre* cohort; [B(ii)] there was no difference between genotypes 6 weeks after tamoxifen treatment. In contrast, swim speed recorded in a continuous swim task was lower in *Stop/y,Cre* mice pre- and post-tamoxifen treatment [C(i) and (ii)]. Performance on the

performance after treatment ($P < 0.05$). Thus, *Stop/y,Cre* mice benefited considerably more from the treatment than controls and although sensory-motor skill is fully restored for simpler/wider beams, it is not fully rescued to wild-type levels.

Loss of muscle strength, possibly related to degeneration of spinal cord motor neurons (Oldfors *et al.*, 1988) occurs early in the Rett syndrome disease process. This parameter was assessed with a grip-strength meter prior to and following gene reactivation (Fig. 4B) in wild-type and *Stop/y,Cre* mice. The initial grip-strength deficit ($P < 0.05$) in *Stop/y,Cre* mice was fully recovered after tamoxifen injections. Indeed, no phenotype was detectable 5 weeks post-treatment [Fig. 4B(ii)] [interaction of genotype and test-phase (before and after treatment) as factors, $P < 0.05$; for *post hoc*, see asterisks in Fig. 4B]. This was due in part to a reduction of grip strength in wild-type ($P < 0.05$) but also to a reliable improvement in grip strength in *Stop/y,Cre* mice post-reactivation ($P < 0.05$). Three further measures pertaining to motor movement and muscle strength were undertaken. Firstly, mice were tested on the rotating rod so that they were compelled to progress in order to avoid falling off. The latency time until descent was initially recorded for all trials, and then converted into rotations per min (rpm) sustained during each trial/session (Fig. 4D). While genotypes differed significantly during pretreatment for both compound measures [Fig. 4D(i)] (overall two-way ANOVA, main effect of genotype $P < 0.05$, *post hoc* $P < 0.05$; n.s. for post-treatment results), tamoxifen exposure completely rescued this phenotype and there was no difference between groups after treatment [Fig. 4D(ii)]. This was due to an improvement of *Stop/y,Cre* mice after treatment ($P < 0.05$) while wild-type did not change. Similar results were obtained for motor learning indexed as improvement from Trial 1 to Trial 8. Although both genotypes presented with motor learning (wild-type: $P < 0.05$; *Stop/y,Cre*: $P < 0.05$), performance was lower for *Stop/y,Cre* mice (Fig. 4E) pre- but not post-treatment suggesting complete rescue of this phenotype. As a second paradigm for enforced movement, we determined swim speed recorded in a water maze during a 30 s swim period (Fig. 4C). In line with the rotarod results, *Stop/y,Cre* mice swam slower than wild-type ($P < 0.05$ for genotype, no interaction with test phase). The pretreatment difference [Fig. 4C(i), $P < 0.05$] persisted after *Mecp2* gene activation [Fig. 4C(ii); $P < 0.05$], but there was a significant improvement in this marker from pre- to post-treatment in *Stop/y,Cre* mice ($P < 0.05$), but no change in wild-type. These findings add support to the notion that late restoration of MeCP2 leads to recovery of movement-related disabilities. To further test aspects of motor function we conducted a

rotarod was significantly reduced for maximum attained rotation speed [D(i)] and for motor learning [E(i)] in *Stop/y,Cre* mice pretreatment. This phenotype fully recovered following tamoxifen administration [D(ii) and E(ii)]. Not affected by treatment were parameters of gait as determined by CatWalk. There was a shorter stride length for all paws [F(i) and (ii)] and greater paw distance between the hind, but not front legs [G(i) and (ii)], both pre- and post-treatment, respectively. Means \pm SEM. Asterisks indicate $P < 0.05$ relative to wild-type.

gait analysis. Front/hind paw stride length (Fig. 4F) and paw width (Fig. 4G) measures were obtained using the CatWalk (see 'Materials and methods' section). Both markers were reliably different between genotypes [Fig. 4F(i) and 4G(i)], suggesting that a wider hind paw width leads to smaller stride length in *Stop/y,Cre* mice. Interestingly, these phenotypes were not recovered after tamoxifen treatment [Fig. 4F(ii) and 4G(ii)]. It thus appears that neuromuscular defects affecting gait may be less reversible by *Mecp2* gene activation than other aspects of the phenotype or take longer to recover.

Discussion

Structural plasticity in the Rett syndrome brain

Neurobiological orthodoxy holds that structural abnormalities arising from abnormal brain development result in a range of neurological and psychiatric symptoms that are essentially irreversible in adults. Hence Rett syndrome is routinely classified as a neurodevelopmental disorder on the assumption that MeCP2-deficiency during development is at the root of this condition. Several phenotypes such as disturbances in calcium homeostasis in cultured neurons (Mironov *et al.*, 2009) are evident at early developmental time points in *Mecp2*-null mice and early neuronal defects are also detected in induced pluripotent stem cells derived from patients with Rett syndrome (Marchetto *et al.*, 2010; Cheung *et al.*, 2011). Moreover, various clinical studies report discrete alterations in the pre-symptomatic phase (Charman *et al.*, 2002) while early effects have also been seen in *Mecp2* mutant mice (Picker *et al.*, 2006; Santos *et al.*, 2007; De Filippis *et al.*, 2010). Against this conventional classification however, functional studies in a range of animal models, including our previous work on MeCP2-deficient mice (Guy *et al.*, 2007), demonstrate that reversing or compensating for some of the underlying molecular deficits in adult mice can result in substantial improvements in function (Ehninger *et al.*, 2008). In particular, almost complete reversal of Rett syndrome-like symptoms was observed in females heterozygous for a *Mecp2*-STOP allele even though the animals were >6 months old and therefore long past any known developmental event. The implication of these findings is that development in the absence of MeCP2 does not irreversibly compromise all subsequent brain function. In short, they suggest that Rett syndrome may defy simple classification as a neurodevelopmental disorder. A potential caveat to this revisionist view could be that reversal applies only to superficial features of the Rett syndrome-like phenotype, leaving fundamental aspects of neurological function in the original defective state. In our earlier study, reversal of impaired survival, obesity and hippocampal long-term potentiation were assessed quantitatively, but other aspects of phenotype, including gait, breathing, mobility, tremor and general condition were assayed using a 'light touch' observational protocol that could be applied on a weekly basis over many months (Guy *et al.*, 2007). The purpose of the present study was to assess

the reversibility of a range of phenotypic traits in a more robust and quantitative manner.

Although several 'neurodevelopmental disorders' show evidence of a degree of reversal, there have been few studies of the extent to which defects in brain morphology can be structurally repaired *in vivo*. Morphological abnormalities including altered neuronal packing density, altered neuronal size and dendritic complexity have been reported both in human Rett syndrome (Armstrong *et al.*, 1995, 1998; Belichenko *et al.*, 1997; Armstrong, 2005) and MeCP2-deficient animal models (Kishi and Macklis, 2004; Belichenko *et al.*, 2008, 2009a, b; Jentarra *et al.*, 2010). At a gross level the *Stop/y* mouse brain appears relatively normal in terms of lamination and architecture, but at a cellular level we confirmed reduced neuronal size and dendritic length and complexity within the primary motor cortex. All of these defects were significantly improved following *Mecp2* activation, approaching or reaching wild-type levels. We conclude that MeCP2-deficient neurons exhibit considerable structural plasticity even in a nervous system that is fully adult. However, the lack of an available comparison with untreated *Stop/y,Cre* mice (which do not survive), somewhat hinders a straightforward 'treatment-effect' interpretation. These findings nevertheless extend previous studies showing that deficits in dendritic, synaptic and axonal morphologies of MeCP2-deficient neurons are reversible in cultured systems following reintroduction of MeCP2 (Rastegar *et al.*, 2009) or by pharmacological interventions targeting aberrant signalling processes (Larimore *et al.*, 2009; Tropea *et al.*, 2009) or by targeting astrocyte function (Lioy *et al.*, 2011).

A prominent feature of many patients with Rett syndrome is microcephaly. Unlike other neuronal measures, which showed a marked reversal of morphological impairment, the gross measure of neuropil (cortical thickness) was not reversed to a statistically significant extent. Thus structural plasticity at the cellular level may not be mirrored in the surrounding skull. Indeed, we know from previous work that very rapid activation of MeCP2 (over days) is detrimental while a more gradual reactivation regime (over weeks) avoids this lethality (Guy *et al.*, 2007). The possibility that abrupt remodelling of the nervous system within the confines of a microencephalic skull is deleterious and remains to be investigated.

Delayed activation of MeCP2 stabilizes respiratory function

Breathing abnormalities are a prominent feature of Rett syndrome, including irregular respiratory patterns during wakefulness, breath holding, sighs and apnoeas (Julu *et al.*, 2001). Whole body plethysmography confirmed the presence of an overt breathing phenotype in the *Stop/y,Cre* mice, including increased variability of breathing pattern and the increased occurrence of abnormal breaths (Fig. 3). These findings are consistent with similar measures conducted in other *Mecp2*-mutant mouse lines (Viemari *et al.*, 2005; Ogier *et al.*, 2007; Roux *et al.*, 2007; Tropea *et al.*, 2009; Abdala *et al.*, 2010; Pratte *et al.*, 2011). We show here that late activation of the *Mecp2* gene generates a robust improvement in breathing patterns in the mice with Rett syndrome, including a near complete reversal of breathing pattern

dysrhythmias and reduced incidence of abnormal sigh-like breaths. The brainstem pathology underlying the Rett syndrome respiratory phenotype is not fully understood but has been the subject of intensive research particularly testing putative pharmacological therapies. Previous studies have shown improvement of respiratory rhythm in *Mecp2*-null male mice by application of desipramine to target the noradrenergic system (Roux *et al.*, 2007) or in MeCP2-deficient female mice by combining a GABA reuptake blocker with a 5HT1a agonist (Abdala *et al.*, 2010). Taken together with the results of this study and the recent report by Lioy and colleagues (2011) focusing on astrocyte function, the respiratory phenotype may be a therapeutically tractable feature of Rett syndrome.

Sensory-motor dysfunction is rescued by late *Mecp2* gene activation

A number of studies have previously characterized changes in performance in similar tasks in a number of MeCP2-mutant lines (Stearns *et al.*, 2007; Kondo *et al.*, 2008; Pratte *et al.*, 2011) and our findings in the *Stop/y* hemizygous mouse were consistent with deficits seen in *Mecp2*-null studies. Following reactivation of *Mecp2* there was evidence for modest but significant improvement across a wide range of motor and locomotor tasks. We did not attempt to directly relate observed morphological changes in motor cortex with functional effects that presumably involve a range of brain structures/circuits. It is clear however, that late reactivation of the *Mecp2* gene caused a quantitative improvement in several motor functions including coordination and balance (rotarod and balance beam). Also muscular strength was restored to almost wild-type levels. Swim speed increased after *Mecp2* gene activation, but remained significantly lower than wild-type. Least reversible were defects in gait, which persisted at significant levels in otherwise 'rescued' animals. Failure to fully reverse symptoms could be taken as evidence that some defects are not rectified by restoration of MeCP2. It is also possible that some phenotypes may show a more protracted or delayed rescue than others. There are, however, two confounding issues that qualify this interpretation. Firstly, activation affects 70% of brain cells on average, leaving 30% highly deficient in MeCP2. We do not know that all phenotypes can be rectified by such a mosaic genetic rescue. Secondly, due to limited survival of *Stop/y* animals, unreversed mice were not available for testing 5 weeks after tamoxifen treatment. This means that mutant mice before and after gene reactivation were compared with wild-type littermates. The results were unambiguous in cases where the defect was fully reversed to the wild-type level, but the defect that persists, abnormal gait, was less easy to interpret. This difficulty arises because *Stop/y,Cre* animals were relatively mildly affected when the experiment began. Therefore, a parameter that appears to remain unchanged relative to wild-type after *Mecp2* activation is being compared with that of a weakly symptomatic animal and does not take into account the phenotypic decline that follows. Persistence of a phenotypic feature in the *Mecp2*-reactivated animals may therefore represent significant stabilization of a sign that would almost certainly have become progressively more severe

during the lifetime of the animal. Indeed, a recent study in which deletion of *Mecp2* in the adult mouse recapitulates the phenotype of germ line knockout of *Mecp2* would support the line that MeCP2 has a necessary role beyond development and throughout adult life (McGraw *et al.*, 2011). In a clinical neurology context, this report coupled with the current findings suggest that therapeutic amelioration of features associated with MeCP2 insufficiency may be clinically achievable, but with the possible exception of gene replacement therapy, any potential treatment may need to be lifelong rather than transient therapeutic intervention delivered during a critical or sensitive periods of development.

In summary, we have measured reversibility of fundamental aspects of the *Stop/y* phenotype and find that the great majority become significantly less severe when MeCP2 is restored in ~70% of cells. Importantly, neuronal morphology is rectified, indicating significant plasticity in the adult mouse. Our findings suggest that a ~25-fold reduction in the level of MeCP2 during brain development has no lasting consequences, as late administration of MeCP2 can reverse the observed defects. It has previously been suggested that MeCP2 is not required for brain development, but plays a role in maintaining neurological function once development is complete (Guy *et al.*, 2001, 2007; Kishi and Macklis, 2004). The current findings sustain this and they highlight the need for a more complete description of the role played by MeCP2 in brain cell homeostasis.

Acknowledgements

We are grateful to Helene Cheval for helpful comments on the article and to Sarah Barry for statistics advice.

Funding

Medical Research Council (G0800401); Wellcome Trust; Scottish Rett Syndrome Association and Rett Syndrome Research Trust.

Supplementary material

Supplementary material is available at *Brain* online.

References

- Abdala AP, Dutschmann M, Bissonnette JM, Paton JF. Correction of respiratory disorders in a mouse model of Rett syndrome. *Proc Natl Acad Sci USA* 2010; 107: 18208–13.
- Amir RE, Van den Veyver IB, Wan M, Tran CQ, Francke U, Zoghbi HY. Rett syndrome is caused by mutations in X-linked MECP2, encoding methyl-CpG-binding protein 2. *Nat Genet* 1999; 23: 185–8.
- Armstrong DD. Can we relate MeCP2 deficiency to the structural and chemical abnormalities in the Rett brain? *Brain Dev* 2005; 27 (Suppl. 1): S72–6.
- Armstrong D, Dunn JK, Antalffy B, Trivedi R. Selective dendritic alterations in the cortex of Rett syndrome. *J Neuropathol Exp Neurol* 1995; 54: 195–201.

- Armstrong DD, Dunn K, Antalffy B. Decreased dendritic branching in frontal, motor and limbic cortex in Rett syndrome compared with trisomy 21. *J Neuropathol Exp Neurol* 1998; 57: 1013–7.
- Asaka Y, Jugloff DG, Zhang L, Eubanks JH, Fitzsimonds RM. Hippocampal synaptic plasticity is impaired in the Mecp2-null mouse model of Rett syndrome. *Neurobiol Dis* 2006; 21: 217–27.
- Belichenko NP, Belichenko PV, Li HH, Mobley WC, Francke U. Comparative study of brain morphology in Mecp2 mutant mouse models of Rett syndrome. *J Comp Neurol* 2008; 508: 184–95.
- Belichenko NP, Belichenko PV, Mobley WC. Evidence for both neuronal cell autonomous and nonautonomous effects of methyl-CpG-binding protein 2 in the cerebral cortex of female mice with Mecp2 mutation. *Neurobiol Dis* 2009a; 34: 71–7.
- Belichenko PV, Hagberg B, Dahlstrom A. Morphological study of neocortical areas in Rett syndrome. *Acta Neuropathol* 1997; 93: 50–61.
- Belichenko PV, Oldfors A, Hagberg B, Dahlstrom A. Rett syndrome: 3-D confocal microscopy of cortical pyramidal dendrites and afferents. *Neuroreport* 1994; 5: 1509–13.
- Belichenko PV, Wright EE, Belichenko NP, Masliah E, Li HH, Mobley WC, et al. Widespread changes in dendritic and axonal morphology in Mecp2-mutant mouse models of Rett syndrome: evidence for disruption of neuronal networks. *J Comp Neurol* 2009b; 514: 240–58.
- Chao HT, Zoghbi HY, Rosenmund C. MeCP2 controls excitatory synaptic strength by regulating glutamatergic synapse number. *Neuron* 2007; 56: 58–65.
- Charman T, Cass H, Owen L, Wigram T, Slonims V, Weeks L, et al. Regression in individuals with Rett syndrome. *Brain Dev* 2002; 24: 281–3.
- Chen RZ, Akbarian S, Tudor M, Jaenisch R. Deficiency of methyl-CpG binding protein-2 in CNS neurons results in a Rett-like phenotype in mice. *Nat Genet* 2001; 27: 327–31.
- Cheung AY, Horvath LM, Grafodatskaya D, Pasceri P, Weksberg R, Hotta A, et al. Isolation of MECP2-null Rett syndrome patient hiPS cells and isogenic controls through X-chromosome inactivation. *Hum Mol Genet* 2011; 20: 2103–15.
- Dani VS, Chang Q, Maffei A, Turrigiano GG, Jaenisch R, Nelson SB. Reduced cortical activity due to a shift in the balance between excitation and inhibition in a mouse model of Rett syndrome. *Proc Natl Acad Sci USA* 2005; 102: 12560–5.
- D'Cruz JA, Wu C, Zahid T, El-Hayek Y, Zhang L, Eubanks JH. Alterations of cortical and hippocampal EEG activity in MeCP2-deficient mice. *Neurobiol Dis* 2010; 38: 8–16.
- De Filippis B, Ricceri L, Laviola G. Early postnatal behavioral changes in the Mecp2-308 truncation mouse model of Rett syndrome. *Genes Brain Behav* 2010; 9: 213–23.
- Ehninger D, Li W, Fox K, Stryker MP, Silva AJ. Reversing neurodevelopmental disorders in adults. *Neuron* 2008; 60: 950–60.
- Guy J, Gan J, Selfridge J, Cobb S, Bird A. Reversal of neurological defects in a mouse model of Rett syndrome. *Science* 2007; 315: 1143–7.
- Guy J, Hendrich B, Holmes M, Martin JE, Bird A. A mouse Mecp2-null mutation causes neurological symptoms that mimic Rett syndrome. *Nat Genet* 2001; 27: 322–6.
- Jentarra GM, Olfers SL, Rice SG, Srivastava N, Homanics GE, Blue M, et al. Abnormalities of cell packing density and dendritic complexity in the MeCP2 A140V mouse model of Rett syndrome/X-linked mental retardation. *BMC Neurosci* 2010; 11: 19.
- Julu PO, Kerr AM, Apartopoulos F, Al-Rawas S, Engerstrom IW, Engerstrom L, et al. Characterisation of breathing and associated central autonomic dysfunction in the Rett disorder. *Arch Dis Child* 2001; 85: 29–37.
- Katz DM, Dutschmann M, Ramirez JM, Hilaire G. Breathing disorders in Rett syndrome: progressive neurochemical dysfunction in the respiratory network after birth. *Respir Physiol Neurobiol* 2009; 168: 101–8.
- Kishi N, Macklis JD. MECP2 is progressively expressed in post-migratory neurons and is involved in neuronal maturation rather than cell fate decisions. *Mol Cell Neurosci* 2004; 27: 306–21.
- Kline DD, Ogier M, Kunze DL, Katz DM. Exogenous brain-derived neurotrophic factor rescues synaptic dysfunction in Mecp2-null mice. *J Neurosci* 2010; 30: 5303–10.
- Kondo M, Gray LJ, Pelka GJ, Christodoulou J, Tam PP, Hannan AJ. Environmental enrichment ameliorates a motor coordination deficit in a mouse model of Rett syndrome–Mecp2 gene dosage effects and BDNF expression. *Eur J Neurosci* 2008; 27: 3342–50.
- Larimore JL, Chapeau CA, Kudo S, Theibert A, Percy AK, Pozzo-Miller L. Bdnf overexpression in hippocampal neurons prevents dendritic atrophy caused by Rett-associated MECP2 mutations. *Neurobiol Dis* 2009; 34: 199–211.
- Lioy DT, Garg SK, Monaghan CE, Raber J, Foust KD, Kaspar BK, et al. A role for glia in the progression of Rett's syndrome. *Nature* 2011; 475: 497–500.
- Luikenhuis S, Giacometti E, Beard CF, Jaenisch R. Expression of MeCP2 in postmitotic neurons rescues Rett syndrome in mice. *Proc Natl Acad Sci USA* 2004; 101: 6033–8.
- Maliszewska-Cyna E, Bawa D, Eubanks JH. Diminished prevalence but preserved synaptic distribution of N-methyl-d-aspartate receptor subunits in the methyl CpG binding protein 2 (MeCP2)-null mouse brain. *Neuroscience* 2010; 168: 624–32.
- Marchetto MC, Carroumeu C, Acab A, Yu D, Yeo GW, Mu Y, et al. A model for neural development and treatment of Rett syndrome using human induced pluripotent stem cells. *Cell* 2010; 143: 527–39.
- McGraw CM, Samaco RC, Zoghbi HY. Adult neural function requires MeCP2. *Science* 2011; 333: 186.
- McNair K, Spike R, Guilding C, Prendergast GC, Stone TW, Cobb SR, et al. A role for RhoB in synaptic plasticity and the regulation of neuronal morphology. *J Neurosci* 2010; 30: 3508–17.
- Medrihan L, Tantalaki E, Aramuni G, Sargsyan V, Dudanova I, Missler M, et al. Early defects of GABAergic synapses in the brain stem of a MeCP2 mouse model of Rett syndrome. *J Neurophysiol* 2008; 99: 112–21.
- Mironov SL, Skorova E, Hartelt N, Mironova LA, Hasan MT, Kugler S. Remodelling of the respiratory network in a mouse model of Rett syndrome depends on brain-derived neurotrophic factor regulated slow calcium buffering. *J Physiol* 2009; 587 (Pt 11): 2473–85.
- Moretti P, Levenson JM, Battaglia F, Atkinson R, Teague R, Antalffy B, et al. Learning and memory and synaptic plasticity are impaired in a mouse model of Rett syndrome. *J Neurosci* 2006; 26: 319–27.
- Moretti P, Zoghbi HY. MeCP2 dysfunction in Rett syndrome and related disorders. *Curr Opin Genet Dev* 2006; 16: 276–81.
- Nelson ED, Kavalali ET, Monteggia LM. Activity-dependent suppression of miniature neurotransmission through the regulation of DNA methylation. *J Neurosci* 2008; 28: 395–406.
- Neul JL, Kaufmann WE, Glaze DG, Christodoulou J, Clarke AJ, Bahi-Buisson N, et al. Rett syndrome: revised diagnostic criteria and nomenclature. *Ann Neurol* 2010; 68: 944–50.
- Nomura Y, Segawa M. Motor symptoms of the Rett syndrome: abnormal muscle tone, posture, locomotion and stereotyped movement. *Brain Dev* 1992; 14 (Suppl.): S21–8.
- Ogier M, Wang H, Hong E, Wang Q, Greenberg ME, Katz DM. Brain-derived neurotrophic factor expression and respiratory function improve after ampakine treatment in a mouse model of Rett syndrome. *J Neurosci* 2007; 27: 10912–7.
- Oldfors A, Hagberg B, Nordgren H, Sourander P, Witt-Engerstrom I. Rett syndrome: spinal cord neuropathology. *Pediatr Neurol* 1988; 4: 172–4.
- Picker JD, Yang R, Ricceri L, Berger-Sweeney J. An altered neonatal behavioral phenotype in Mecp2 mutant mice. *Neuroreport* 2006; 17: 541–4.
- Pratte M, Panayotis N, Ghata A, Villard L, Roux JC. Progressive motor and respiratory metabolism deficits in post-weaning Mecp2-null male mice. *Behav Brain Res* 2011; 216: 313–20.
- Rastegar M, Hotta A, Pasceri P, Makarem M, Cheung AY, Elliott S, et al. MECP2 isoform-specific vectors with regulated expression for Rett syndrome gene therapy. *PLoS One* 2009; 4: e6810.

- Roux JC, Dura E, Moncla A, Mancini J, Villard L. Treatment with desipramine improves breathing and survival in a mouse model for Rett syndrome. *Eur J Neurosci* 2007; 25: 1915–22.
- Santos M, Silva-Fernandes A, Oliveira P, Sousa N, Maciel P. Evidence for abnormal early development in a mouse model of Rett syndrome. *Genes Brain Behav* 2007; 6: 277–86.
- Stearns NA, Schaevitz LR, Bowling H, Nag N, Berger UV, Berger-Sweeney J. Behavioral and anatomical abnormalities in *Mecp2* mutant mice: a model for Rett syndrome. *Neuroscience* 2007; 146: 907–21.
- Taneja P, Ogier M, Brooks-Harris G, Schmid DA, Katz DM, Nelson SB. Pathophysiology of locus ceruleus neurons in a mouse model of Rett syndrome. *J Neurosci* 2009; 29: 12187–95.
- Tropea D, Giacometti E, Wilson NR, Beard C, McCurry C, Fu DD, et al. Partial reversal of Rett syndrome-like symptoms in *MeCP2* mutant mice. *Proc Natl Acad Sci USA* 2009; 106: 2029–34.
- Viemari JC, Roux JC, Tryba AK, Saywell V, Burnet H, Pena F, et al. *Mecp2* deficiency disrupts norepinephrine and respiratory systems in mice. *J Neurosci* 2005; 25: 11521–30.
- Weng SM, McLeod F, Bailey ME, Cobb SR. Synaptic plasticity deficits in an experimental model of Rett syndrome: long-term potentiation saturation and its pharmacological reversal. *Neuroscience* 2011; 180: 314–21.
- Zhang L, He J, Jugloff DG, Eubanks JH. The *MeCP2*-null mouse hippocampus displays altered basal inhibitory rhythms and is prone to hyperexcitability. *Hippocampus* 2008; 18: 294–309.